P-ISSN 1991-8941
E-ISSN 2706-6703
Vol. 19, No. 2 (2025)

Journal of University of Anbar for Pure Science
(JUAPS)

journal homepage: juaps.uoanbar.edu.iq

Open Access

Original Paper

Effect of pH on the structural, morphological, and optical properties of cerium oxide nano-thin films prepared by the hydrothermal method

Abd alhameed A. Hameed [1*], Isam M. Ibrahim [2], J. F. Mohammad [3]

[1]Ministry of Education, Education Direction in Al-Anbar, Iraq
[2]Department of Physics, College of Science, University of Baghdad, Baghdad, Iraq
[3]Physics Department, College of Education for Pure Sciences, University of Anbar, Iraq

ARTICLE INFO

Received: 22/09/2024
Accepted: 22/12/2024
Available online: 14/11/2025
December Issue
10.37652/juaps.2024.153787.1320

Cite @ JUAPS

Corresponding author
Abd alhameed A. Hameed
abd21u3009@uoanbar.edu.iq

ABSTRACT

Cerium oxide (CeO_2) Nano-thin films on a seed layer were synthesized via the hydrothermal method at pH 3 and 9. The structural, morphological, and optical characteristics of the produced films were investigated. X-ray diffraction (XRD) tests showed that the prepared films are polycrystalline and have a cubic structure. Additionally, they have a crystallite size of approximately 14.5 nm and a pH of 3. Increasing the pH to 9 reduced the crystallite size to 12.9 nm. Field-emission scanning electron microscopy (FESEM) images revealed that changing the pH resulted in a reduction in the size of the nanoparticles, while maintaining their spherical shape. Energy-dispersive X-ray Spectroscopy (EDS) analysis confirmed the absence of impurity elements in the prepared samples, verifying the formation of pure cerium oxide. UV-vis examinations showed that increasing the pH value of the prepared films enhanced the optical transmittance and increased the values of the optical energy gap.

Keywords: *CeO_2 films, Hydrothermal method, Nanostructure, Seed layer*

1 INTRODUCTION

Metal oxide thin films have become increasingly popular in various fields, including microelectronics and optics. In addition to its extended lifespan, non-toxicity, and high conductivity, semiconductor metal oxide (SMO) offers various benefits, including low cost, ease of production, and low detection limits for gases. Furthermore, due to their excellent electrical conductivity, large energy gaps, and high optical transparency in the visible spectrum, transparent metal oxide films are highly attractive from a technological standpoint [1–3]. Numerous studies have focused on nanostructured materials because of their purportedly distinct structure and physical characteristics related to grain boundaries and size-dependent non-stoichiometry [4]. Numerous investigations have demonstrated that materials with a grain size of less than 100 nm exhibit distinct properties compared to conventional microcrystalline specimens, including their optical, electrical, mechanical, and catalytic capabilities. Cerium oxide (ceria) films have garnered attention due to their high transparency in the visible and near-infrared regions and their electro-optical performance [4,5]. CeO_2 is a rare-earth oxide with a cubic fluorite structure that offers lots of room for oxygen vacancies to develop and move. CeO_2 has a high concentration of oxygen vacancies and also shows good chemical and physical stability. Furthermore, it exhibits strong catalytic activity due to the simple redox transition between Ce^{+3} and Ce^{+4}. Due to their strong ionic conductivity and/or catalytic activity, CeO_2-based materials are suitable choices for electrodes and/or electrolytes [6, 7]. Cerium oxide, also known as ceria, is a highly attractive metal oxide that has garnered greater attention over the last decade due to its unique and intriguing properties, which include high hardness, UV absorption, reactivity, and exceptional stability at high temperatures [8]. Most novel techniques, including flame spray pyrolysis, hydrothermal synthesis, sol-gel

procedures, combustion synthesis, and a sophisticated thermos-decomposition technique, were employed to generate CeO_2 nanoparticles [9]. There are disadvantages to any preparation technique, including the requirement for a vacuum environment, complicated steps, and high temperatures that may result in impurities, insufficient dispersion, or decreased crystallinity. A synthetic process that employs a bottom-up approach, known as the hydrothermal technique, has become increasingly popular as the method of choice for creating nanomaterials. Its simple process, capacity to create crystals of excellent quality, easy control over shape, effective sintering activity, and low-temperature requirements are mostly to blame for this. Numerous methods for producing CeO_2 nanostructures have been documented in the literature [10–12]. Thus, creating nanostructures with precise control over their size, shape, and chemical composition remains a difficult task [13]. In this study, a hydrothermal method was used to prepare cerium oxide films at different pH values. The effect of pH on the structural, morphological, and optical properties of the resulting solutions was studied.

2 MATERIALS AND METHODS

A hydrothermal method was used to create ceria-thin films on the seeded layer. Initially, distilled water and ethanol were used to thoroughly clean the glass slides in an ultrasonic bath for 10 min. Then, 0.01 M of hydrated cerium chloride ($CeCl_3.7H_2O$) was dissolved in distilled water at room temperature using a magnetic stirrer for 1 h. Using chemical spray pyrolysis at 400 °C, the solution was sprayed onto glass substrates. Five seconds of spraying were followed by a 20-second break. The next step, the growth solution for cerium oxide (CeO_2) films, was prepared by dissolving 0.1 M cerium chloride ($CeCl_3$) in deionized water using a magnetic stirrer for 30 mins.

Then, 0.1 M hexamine ($C_6H_{12}N_4$) was dissolved in distilled water using a magnetic stirrer for 30 min. Subsequently, hexamine was added gradually to the cerium chloride solution, and the mixture was stirred for an additional half hour at room temperature. By adding sodium hydroxide (NaOH) solution, the pH was increased from 3 to 9. Subsequently, these solutions were labeled C1 and C2, respectively. Substrates with seeded layers were arranged vertically within the Teflon-lined stainless-steel autoclave after the final mixture was transferred inside. The autoclave was sealed and maintained in a digitally controlled oven for six hours at a steady temperature of 100 °C. The autoclave was then allowed to cool naturally to room temperature. To remove any remaining solid particles or unreacted atoms from the surface, the substrates were rinsed with deionized water. The samples were then dried in an oven at 100 °C for 30 min. The annealing process was performed in a furnace at 400 °C for 1 hour. Once completed, the films were ready for characterization. The crystalline structure of the prepared samples was analyzed using a Shimadzu XRD-6000 X-ray diffractometer with CuKα radiation (wavelength = 0.154 nm) over a 2θ range of 10°–90°. The surface morphology was examined using field emission scanning electron microscopy (FESEM) with an Inspect F50 system (FEI, Netherlands). Elemental composition was determined by energy-dispersive X-ray spectroscopy (EDS). The optical absorption spectra and energy band gaps of the deposited thin films were measured using a Shimadzu UV-1650 PC UV-Vis spectrophotometer in the wavelength range 300–1100 nm.

3 RESULTS AND DISCUSSION

3.1 Structure and morphological properties

The X-ray diffraction (XRD) analysis of cerium oxide films deposited on glass substrates using the hydrothermal method at 100 °C with a reaction time of 6 h. at pH 3 and 9 showed polycrystalline films with a cubic structure. Diffraction peaks appeared at (111), (002), (022), (113), and (004) at 2θ = 28.57°, 33.04°, 47.40°, 56.30°, and 69.61°, with a preferred orientation along the (022) plane. These peaks match cerium oxide, as confirmed by ICSD card 98-005-3995, and are consistent with prior reports [14]. Figure 1 illustrates that the peak intensity decreases as the pH increases. The crystallite size was estimated using the Scherrer equation $D=k\lambda/\beta\cos\theta$, where β stands for the full width at half-maximum (FWHM), θ is the angle of the diffraction peak, and k is the form factor (0.94) [15]. The wavelength of the X-ray source is λ = 0.12347 nm [16]. The average crystallite size was approximately 14.5 nm at pH 3 and decreased to about 12.9 nm at pH 9, as listed in Table 1, in agreement with [17].

The surface morphologies and particle sizes of the prepared cerium oxide films were studied by FESEM. Figure 2 shows that the dominant particle shape at both pH 3 and pH 9 was spherical. The average particle size was approximately 8.52 nm at pH 3; increasing the pH to 9 raised the size to about 14.75 nm. At higher pH levels, smaller crystallites tend to agglomerate, resulting

in larger, less uniform spherical structures than at lower pH levels, consistent with previous studies [14].

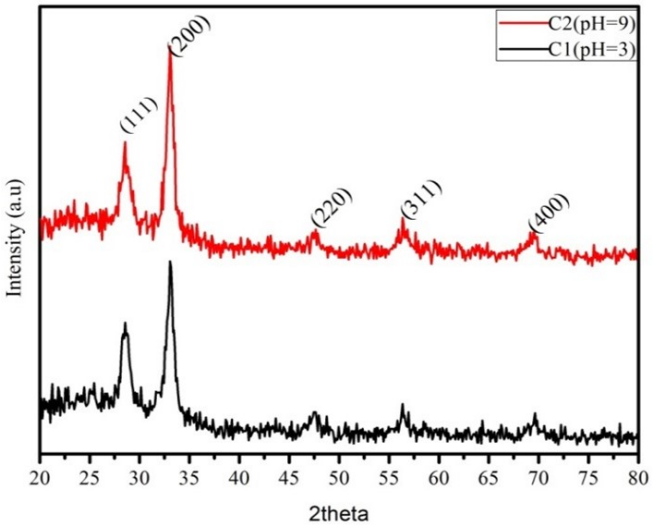

Fig. 1 XRD patterns for CeO_2: C1(pH=3), C2(pH=9)

Table 1 XRD parameters of CeO_2 films

Sample	2θ (Exp.)	d_{hkl} Exp.(A)	d_{hkl} Std.(A)	FWHM	D (nm)
C1 pH=3	28.57	3.12202	3.12347	0.91	8.71
	33.04	2.70894	2.705	0.899	8.63
	47.4	1.91465	1.91272	2	2.96
	56.3	1.63232	1.63118	1.8	3.65
	69.61	1.34961	1.3525	0.24	48.5
C2 pH=9	28.58	3.12003	3.12347	1.2034	7.11
	33.03	2.70959	2.705	0.9181	9.46
	47.57	1.90981	1.91272	0.9539	6.80
	56.37	1.63084	1.63118	0.2685	29.0
	69.39	1.35328	1.3525	0.8391	12

Figure 3 presents the cross-sectional FESEM image, showing a CeO_2 film thickness of approximately 772.2 nm. Thickness was calculated as the average of four measurements: (987 + 585.7 + 700 + 816.1)/4 = 772.2 nm.

Figure 4 presents the EDS results for the cerium oxide (CeO_2) films prepared using the hydrothermal method at different pH values (3 and 9). Sample C1 (pH = 3), cerium (Ce) appears at a lower concentration compared to oxygen. An acidic pH contributes to a higher interaction between cerium and oxygen, leading to the rapid formation of cerium oxides (such as CeO_2). Sample C2 (pH = 9) showed a very low cerium content (8.62%), whereas oxygen was present at a much higher percentage, as shown in Table 2. This suggests that most of the cerium in this sample has been oxidized to form CeO_2, resulting in a higher oxygen concentration detected in the analysis. The elevated oxygen content at pH 9 can be attributed to the nearly complete oxidation of cerium into CeO_2, resulting in a higher observed oxygen percentage in the analysis. In contrast, sample C1 exhibited a higher cerium content due to a less intense reaction with oxygen.

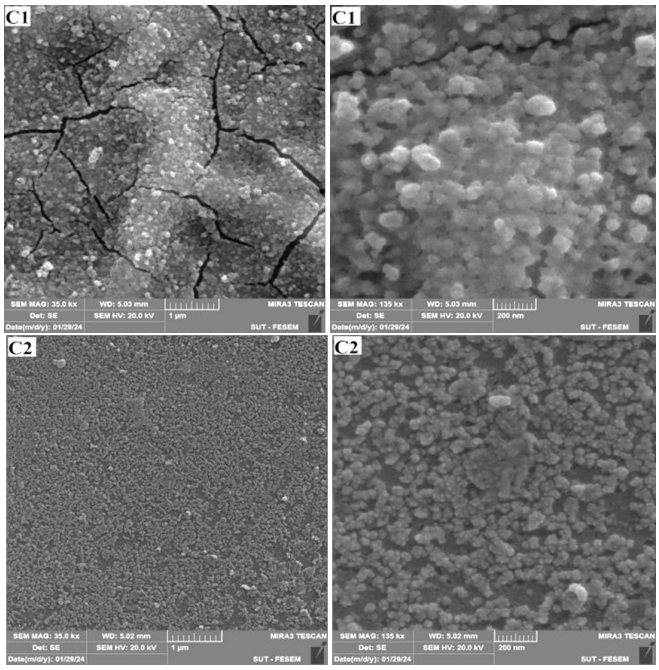

Fig. 2 FESEM of CeO_2 , C1(pH=3) ,C2(pH=9)

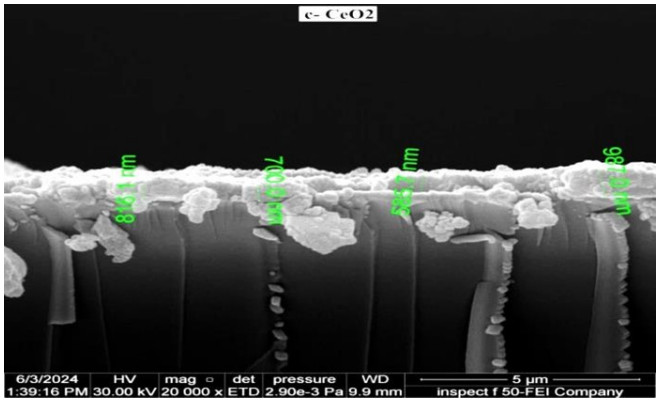

Fig. 3 Cross-sectional FESEM images of CeO_2 films at pH=3

Table 2 Atomic and weight percent ratios of Ce and O for samples, C1, C2

Sample	Element	Weight%	Atomic %
Cl (pH = 3)	Ce	71.71	22.45
	O	28.29	77.55
C 2 (pH = 9)	Ce	8.62	98.93
	O	91.38	1.07

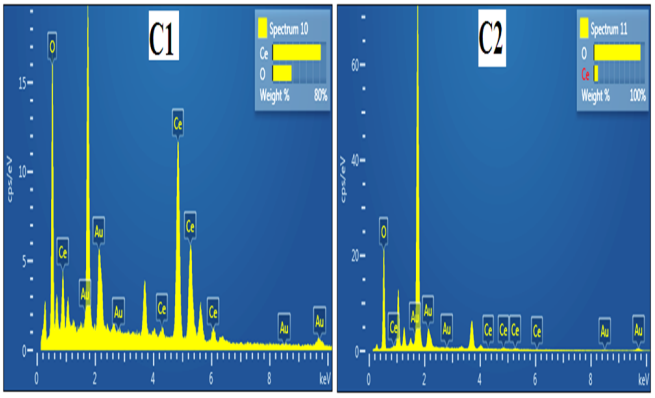

Fig. 4 EDS results of CeO_2, C1(pH=3), C2 (pH=9)

3.2 Optical properties

The optical transmittance of cerium oxide (CeO_2) films prepared by hydrothermal treatment at various pH values is plotted as a function of wavelength in Figure 5. The graph illustrates how changes in pH affect optical transmittance. At pH = 9 (C2), the transmittance was significantly higher across most wavelength ranges compared to pH = 3 (C1). This indicates that alkaline conditions (high pH) result in materials that are more transparent to light. Thus, increasing the pH enhances the optical transmittance of these materials, making them suitable for applications requiring high transparency at specific wavelengths.

The direct optical energy gap for CeO_2 films was calculated using the equation indicated in [18, 19].

$$\alpha h\nu = B\left(h\nu - E_{opt}\right)^{r}$$

Here, B is inversely related to the degree of amorphousness, and E_{opt} represents the optical energy gap. The value of r can be $1/2, 3/2, 2$, or 3 , depending on the type of electronic transition causing the absorption.

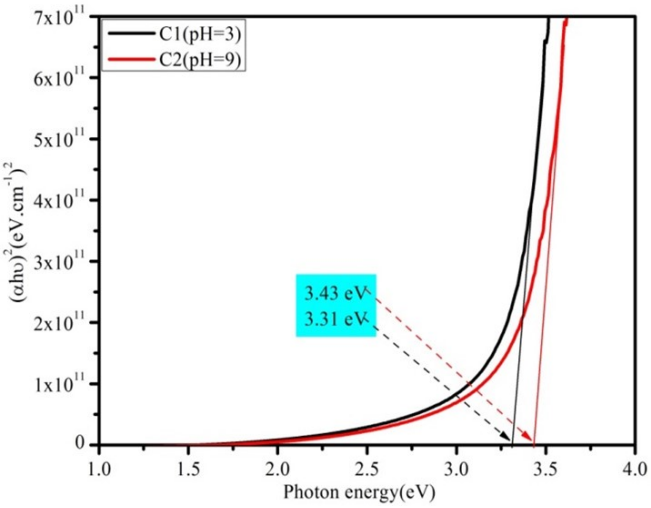

Fig. 5 Optical transmittance of prepared CeO_2 films at different pH values 3 and 9

These values correspond to indirectly allowed transitions, direct transitions, forbidden direct transitions, and forbidden indirect transitions, respectively [16, 20]. By plotting the relationship between $(\alpha h\nu)^2$ and the photon energy $(h\nu)$ and determining the value of the direct optical energy gap (E_g) by extending the straight line of the curve, as shown in Figure 5. It can be observed that the energy gap value for the films prepared at pH 3 was approximately 3.31 eV , while the energy gap value for the films prepared at pH 9 was around 3.43 eV . The increase in pH led to an increase in the values of the optical energy gap, which is consistent with the results demonstrated by [14].

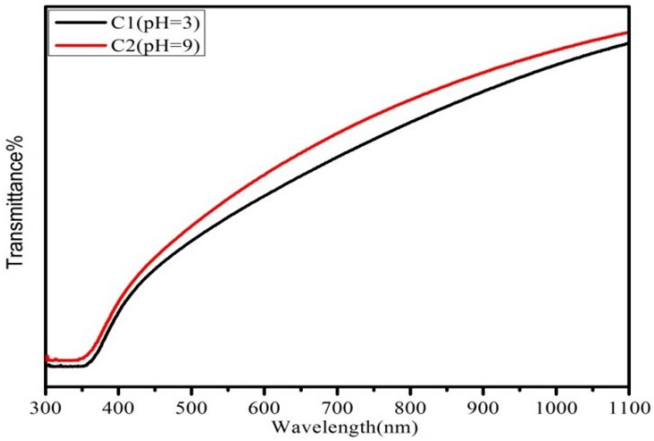

Fig. 6 Optical energy gaps of the prepared CeO_2 films at pH 3 and 9

4 CONCLUSION

Cerium oxide nanofilms were synthesized using the hydrothermal method at pH levels of 3 and 9. The results of the structural examinations revealed that the particles have a spherical shape and are nano-sized, as observed in the prepared films, and exhibit a change in response to variations in the pH value. Additionally, EDS tests showed that all the films contain cerium and oxygen, with no other elements observed. Furthermore, increasing the pH value led to a decrease in the weight ratio of cerium. Optical examinations also revealed that changes in the pH value resulted in increases in both the energy gap and optical transmittance. The above results indicate that the hydrothermal method is suitable for preparing films tailored to the specific application requirements, such as those for detectors or gas sensors.

ACKNOWLEDGEMENT

The Scientific Committee of the Physics Department in the University of Anbar's College of Education for Pure Sciences and the Physics Department in the University of Baghdad's College of Science both support this project.

FUNDING SOURCE

No funds received.

DATA AVAILABILITY

N/A

DECLARATIONS

Conflict of interest

The authors declare that they have no known competing financial interests or personal relationships that could have appeared to influence the work reported in this paper.

Consent to publish

All authors consent to the publication of this work.

Ethical approval

N/A

REFERENCES

[1] Hathal YR, Ibrahim IM, Khalaf MK. Photosensitivity of Nb2O5/Si thin films produced via dc reactive sputtering at different substrate temperatures. Iraqi Journal of Applied Physics. 2024;20(2B):349-56

[2] Hameed AaA, AL-Jumaili HS. Preparation and Characterization of In2O3-CuO Nanocomposite Thin Films as NH3 Gas Sensor. Iraqi Journal of Science. 2021:2204–2212. 10.24996/ijs.2021.62.7.10

[3] Hmeed AaA, Al-Jumaili HS. NO2gas sensor properties of In2O3-CuO Nanocomposite thin films prepared by chemical spray pyrolysis. IOP Conference Series: Materials Science and Engineering. 2021;1095(1):012008. 10.1088/1757-899x/1095/1/012008

[4] Phokha S, Limwichean S, Horprathum M, Patthanasettakul V, Chananonnawathorn C, Eiamchai P, et al. Effect of annealing temperature on the structural and magnetic properties of CeO2 thin films. Thin Solid Films. 2020;704:138001. 10.1016/j.tsf.2020.138001

[5] Gatea HA. Structure and Morphology of CeO2 Nanoparticles Prepared by Hydrothermal Method. International Journal of Thin Film Science and Technology. 2022;11(2):201–206. 10.18576/ijtfst/110207

[6] Liu Z, Wang B, Cazorla C. Mechanical and electronic properties of CeO2 under uniaxial tensile loading: A DFT study. Materialia. 2021;15:101050. 10.1016/j.mtla.2021.101050

[7] Dogdibegovic E, Wang R, Lau GY, Tucker MC. High performance metal-supported solid oxide fuel cells with infiltrated electrodes. Journal of Power Sources. 2019;410–411:91–98. 10.1016/j.jpowsour.2018.11.004

[8] Song X, Zhu W, Wang X, Tan Z. Recent Advances of CeO2-Based Electrocatalysts for Oxygen and Hydrogen Evolution as well as Nitrogen Reduction. ChemElectroChem. 2021;8(6):996–1020. 10.1002/celc.202001614

[9] Soni S, Kumar S, Dalela B, Kumar S, Alvi PA, Dalela S. Defects and oxygen vacancies tailored structural and optical properties in CeO2 nanoparticles doped with Sm3+ cation. Journal of Alloys and Compounds. 2018;752:520–531. 10.1016/j.jallcom.2018.04.157

[10] Meng F, Wang L, Cui J. Controllable synthesis and optical properties of nano-CeO2 via a facile hydrothermal route. Journal of Alloys and Compounds. 2013;556:102–108. 10.1016/j.jallcom.2012.12.096

[11] Meng F, Zhang C, Fan Z, Gong J, Li A, Ding Z, et al. Hydrothermal synthesis of hexagonal CeO2 nanosheets and their room temperature ferromagnetism. Journal of Alloys and Compounds. 2015;647:1013–1021. 10.1016/j.jallcom.2015.06.186

[12] Hassen MM, Ibrahim IM, Abdullah OG, Suhail MH. Improving photodetector performance of PANI nanofiber by adding rare-earth La2O3 nanoparticles. Applied Physics A. 2023;129(2). 10.1007/s00339-023-06415-5

[13] dos Santos APB, Dantas TCM, Costa JAP, Souza LD, Soares JM, Caldeira VPS, et al. Formation of CeO2 nanotubes through different conditions of hydrothermal synthesis. Surfaces and Interfaces. 2020;21:100746. 10.1016/j.surfin.2020.100746

[14] Kareem MT, Hamdan SA. Synthesize and Characterization of Cerium Oxide Nanostructure for Oxidizing Gas Sensor Application. International Academic Journal of Science and Engineering. 2022;9(2):37–45. 10.9756/iajse/v9i2/iajse0912

[15] Ali ZS, Ibrahim IM, Akber HJ. Effect of solvent on hydrothermal synthesis of Cu2ZnSnS4 nanostructures for solar cell applications. In: INTERNATIONAL CONFERENCE OF COMPUTATIONAL METHODS IN SCIENCES AND ENGINEERING ICCMSE 2021. vol. 2611. AIP Publishing; 2023. p. 030010. 10.1063/5.0115474

[16] Farrukh MA, Butt KM, Altaf A, khadim S. Influence of pH and Temperature on Structural, Optical and Catalytical Investigations of CeO2-SiO2 Nanoparticles. Silicon. 2019;11(6):2591–2598. 10.1007/s12633-018-0050-7

[17] Ramachandran M, Subadevi R, Sivakumar M. Role of pH on synthesis and characterization of cerium oxide (CeO2) nano particles by modified co-precipitation method. Vacuum. 2019;161:220–224. 10.1016/j.vacuum.2018.12.002

[18] Afzaal A, Farrukh MA. Zwitterionic surfactant assisted synthesis of Fe doped SnO2-SiO2 nanocomposite with enhanced photocatalytic activity under sun light. Materials Science and Engineering: B. 2017;223:167–177. 10.1016/j.mseb.2017.06.015

[19] Hathal YR, Ibrahim IM, Khalaf MK. Effect of Substrate Temperature on Characteristics and Gas Sensing Properties of Nb2O5/Si Thin Films. Iraqi Journal of Applied Physics. 2024;20(2A):271-7

[20] Pazouki S, Memarian N. Effects of Hydrothermal temperature on the physical properties and anomalous band gap behavior of ultrafine SnO2 nanoparticles. Optik. 2021;246:167843. 10.1016/j.ijleo.2021.167843

How to cite this article

Hameed AA, Ibrahim IM, Mohammad JF. Effect of pH on the structural, morphological, and optical properties of cerium oxide nano-thin films prepared by the hydrothermal method. Journal of University of Anbar for Pure Science. 2025; 19(2):96-101. doi:10.37652/juaps.2024.153787.1320